A MINERALOGICAL SURVEY OF LUNAR CRATER CENTRAL PEAKS WITH MOON MINERALOGY MAPPER DATA: FIRST RESULTS. P. J. Isaacson[1], J. Nettles[1], S. Besse[2], J. Boardman[3], L. Cheek[1], R. Clark[4], D. Dhingra[1], K. Donaldson Hanna[1], J. Head[1], R. Klima[5], G. Kramer[6], U. Mall[7], D. Moriarty[1], J. Mustard[1], N. Petro[8], C. Pieters[1], J. Sunshine[2], L. Taylor[9], S. Tompkins[10], J. Whitten[1], [1]Dept. Geol. Sci., Brown Univ., [Peter_Isaacson@Brown.edu], [2]Univ. of MD, [3]AIG, [4]USGS Denver, [5]JHU/APL, [6]LPI, [7]Max Planck Inst., [8]NASA GSFC, [9]Univ. of TN, [10]DARPA.

Introduction: The compositional structure of the lunar crust is one of the most important and accessible clues to the history of the Moon's thermal and chemical evolution. The variety of new lunar remote sensing datasets offers the opportunity to investigate the global composition of the lunar crust in unprecedented detail. The Moon Mineralogy Mapper (M^3) dataset collected high spectral and spatial resolution visible to near-infrared (VNIR) reflectance spectra in an imaging mode [1]. These combined capabilities make the M^3 dataset ideal for evaluating global surface mineralogy, as the dataset enables investigations of mineralogy with the critical additional element of spatial (and thus geological) context, a capability not provided by spectral profiling instruments that acquire only a single spectrum with each acquisition.

Crater central peaks are ideal for compositional study of the lunar crust for several reasons. First, they expose material from depths generally correlated with their size [2, 3]. Second, their rugged topography generally inhibits the development of a thick regolith layer, making their surfaces appear relatively optically immature, preserving diagnostic spectral absorption features [4-6]. Many previous studies have used central peaks to analyze the composition of the lunar crust [e.g., 7, 8]; we build on these studies by leveraging the additional spatial and spectral capabilities of the M^3 dataset. Here, we illustrate the scope of the project to survey lunar crater central peaks, and present preliminary results for one lunar crater and its surroundings.

Data and Methods: Candidate craters were identified from the lists of craters analyzed by previous studies [7, 8] and from the planetary nomenclature database maintained by the USGS [9, 10]. Mosaics of M^3 data were created through the use of the lunar coordinate information provided with the "backplanes" ("OBS" files) of the M^3 data products. A mosaic was created for each crater, and was sized according to the crater radius plus a buffer to ensure full coverage. Data available to produce these mosaics were in the "K" calibration version of M^3 radiance data [11]. Data from the second M^3 optical period often exhibited substantial errors in spatial registration due to spacecraft operational issues. Newer calibrations will reduce these errors substantially, as discussed in detail by Boardman et al. [12]. A map of the regions used to define the mosaics is presented in Fig. 1.

The Level 1b radiance data were converted to apparent reflectance through correction for the solar flux. Initial spectral analysis focused on the 1 μm region, where preliminary mineralogical assessments can be made with minimal complications. For each apparent reflectance spectrum, a continuum was fit over the 1 μm feature (from 730 to 1580 nm), and the continuum slope removed. A median window filter was applied to perform minor spectral smoothing. For each spectrum, the band minimum wavelength was identified. At that minimum, the depth of the absorption feature was estimated, and the width of the absorption feature was assessed at the half maximum band depth. This process is illustrated in Fig. 2. These parameters were mapped spatially and used to assist in making interpretations about mineralogy. Because this process is performed on image cube mosaics including the crater and its imme-

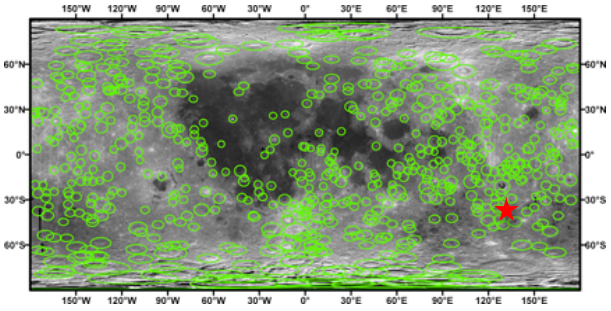

Fig. 1: Map of M^3 image cube mosaics created for this study on Clementine UVVIS ULCN2005 [10] basemap image. Bolyai L, for which results are presented, is indicated by a red star.

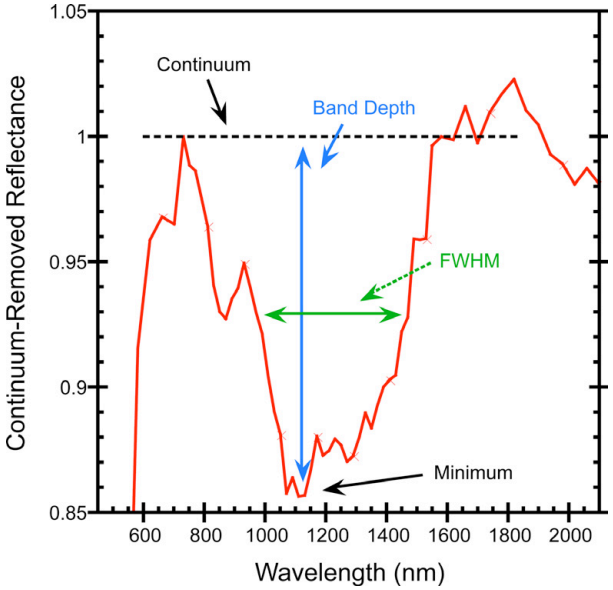

Fig. 2: Method for band minimum and associated parameter calculation. The indicated continuum slope has been removed from this spectrum. Band depth and FWHM are calculated at the band minimum wavelength.

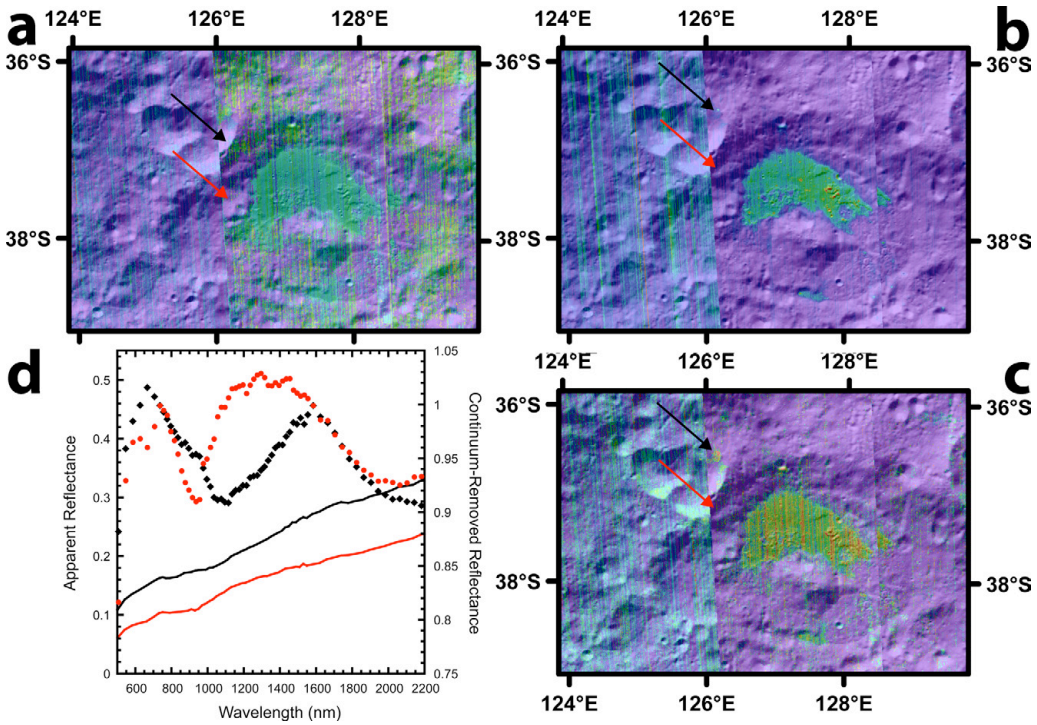

Fig. 3: Example parameter maps for Bolyai L mosaic. The procedure described in Fig. 2 has been applied to each spectrum in this mosaic. (a) Band minimum wavelength (b) Band depth (c) FWHM (d) Example spectra , locations highlighted by red and black arrows. Note the broad, long-wavelength absorption feature in the black spectrum as highlighted by the band parameter maps. Purples and blues represent "low" parameter values, and orange/reds indicate high values.

diate surroundings, our analyses include the crater floor, walls, rim, and often continuous ejecta deposits in addition to the central peak, enabling evaluations of the local geology of a crater rather than just a general, average classification of the central peak itself.

Initial Results, Bolyai L Example: Results are presented here for a single M^3 image cube mosaic, for the crater Bolyai L, located between Mare Australe and the South Pole-Aitken (SPA) basin (Fig. 1). Maps of band minimum, depth, and FWHM are presented in Fig. 3. Bolyai L is a relatively degraded crater, and its central peak is comparatively optically mature, as it does not exhibit substantial differences from the materials surrounding the crater in the parameter maps of Fig. 3. However, this demonstrates the strength of our regional analysis approach; our approach enables us to analyze the geology of the entire crater and its surroundings, rather than restricting us to analyses only of the central peak. The band minimum map (Fig. 3a) is largely dominated by striping ("noise"), although the mare basalt fill in the lower middle portion of the image does exhibit longer-wavelength band minima due to the generally gabbroic (high-Ca pyroxene-rich) compositions typical of mare basalts. The mare fill shows a clear signature in the band depth map (Fig. 3b), as the mare exhibits relatively strong absorption features due to its pyroxene-rich composition. The band width map (Fig. 3c) also shows strong signatures in the basalt fill, although the small point indicated by the black arrow shows a local "high FWHM" anomaly as well. In comparing spectra from the two indicated locations (red and black), the potential of our approach is demonstrated. The local FWHM "hotspot", labeled in black, also seen as a local anomaly in the band depth and, to a lesser extent, the band minimum map, shows clear evidence for a broad, long-wavelength absorption feature consistent with olivine. The small mafic anomaly labeled in red, which does not exhibit a FWHM anomaly, is a more typical low-Ca pyroxene.

Status and Future Work: The analysis approach discussed above is currently being applied to the full set of mosaics illustrated in Fig. 1, which also illustrates the scope of the project. This approach provides results that enable mineralogical interpretations, as demonstrated above. However, the band minimum-finding procedure is sensitive to spectral noise or artifacts, as it is based on single M^3 channels. Subsequent analytical approaches may involve fits to the continuum-removed spectra. This would reduce the noise sensitivity and increase the spectral resolution of the located absorption minimum. However, the above discussion demonstrates the potential of the data and method to provide new insight into the composition of lunar crater central peaks and thus of the compositional structure of the lunar crust.

Acknowledgments: M^3 science validation is supported through NASA contract #NNM05AB26C. M^3 is supported as a NASA Discovery Program mission of opportunity. The M^3 team is grateful to ISRO for the opportunity to fly as a guest instrument on Chandrayaan-1.

References: [1] Pieters, C.M. et al. (2009) *Current Science*, **96**, 500-505. [2] Melosh, H.J. (1989) *Impact cratering: A geologic process*. [3] Cintala, M.J. and Grieve, R.A.F. (1998) *MAPS*, **33**, 889-912. [4] Pieters, C.M. et al. (2000) *MAPS*, **35**, 1101-1107. [5] Hapke, B. (2001) *JGR*, **106**, 10039-10074. [6] Noble, S.K. et al. (2001) *MAPS*, **36**, 31-42. [7] Tompkins, S. and Pieters, C.M. (1999) *MAPS*, **34**, 25-41. [8] Cahill, J.T.S. et al. (2009) *JGR*, **114**, [9] Andersson, L.A. and Whitaker, E.A. (1982) *NASA catalogue of lunar nomenclature*. [10] Archinal, B.A. et al., USGS Open-File Report 2006-1367. [11] Green, R. et al. (2010) *JGR*, In prep. [12] Boardman, J. et al. (2010) *JGR*, Under Review.